Heriot-Watt University
Research Gateway

Rapid combustion synthesis of $Cu_2Y_2O_5$ as a precursor for $CuYO_2$ delafossite

Citation for published version:
Racu, AV, Baies, R, Popuri, SR, Pascariu, M-C, Niculescu, M & Banica, R 2018, 'Rapid combustion synthesis of $Cu_2Y_2O_5$ as a precursor for $CuYO_2$ delafossite', *Materials Today Communications*, vol. 14, pp. 233-239. https://doi.org/10.1016/j.mtcomm.2018.01.010

Digital Object Identifier (DOI):
10.1016/j.mtcomm.2018.01.010

Link:
Link to publication record in Heriot-Watt Research Portal

Document Version:
Peer reviewed version

Published In:
Materials Today Communications

Publisher Rights Statement:
© 2018 Elsevier B.V.

General rights
Copyright for the publications made accessible via Heriot-Watt Research Portal is retained by the author(s) and / or other copyright owners and it is a condition of accessing these publications that users recognise and abide by the legal requirements associated with these rights.

Take down policy
Heriot-Watt University has made every reasonable effort to ensure that the content in Heriot-Watt Research Portal complies with UK legislation. If you believe that the public display of this file breaches copyright please contact open.access@hw.ac.uk providing details, and we will remove access to the work immediately and investigate your claim.

Download date: 16. Sep. 2024

Accepted Manuscript

Title: Rapid combustion synthesis of $Cu_2Y_2O_5$ as a precursor for $CuYO_2$ delafossite

Authors: Andrei V. Racu, Radu Baies, Srinivas R. Popuri, Mihai-Cosmin Pascariu, Mircea Niculescu, Radu Banica

PII: S2352-4928(17)30349-5
DOI: https://doi.org/10.1016/j.mtcomm.2018.01.010
Reference: MTCOMM 269

To appear in:

Received date: 5-1-2018
Accepted date: 11-1-2018

Please cite this article as: Andrei V.Racu, Radu Baies, Srinivas R.Popuri, Mihai-Cosmin Pascariu, Mircea Niculescu, Radu Banica, Rapid combustion synthesis of Cu2Y2O5 as a precursor for CuYO2 delafossite, Materials Today Communications https://doi.org/10.1016/j.mtcomm.2018.01.010

This is a PDF file of an unedited manuscript that has been accepted for publication. As a service to our customers we are providing this early version of the manuscript. The manuscript will undergo copyediting, typesetting, and review of the resulting proof before it is published in its final form. Please note that during the production process errors may be discovered which could affect the content, and all legal disclaimers that apply to the journal pertain.

Rapid combustion synthesis of $Cu_2Y_2O_5$ as a precursor for $CuYO_2$ delafossite

Andrei V. Racu[a,b], Radu Baies[a,c], Srinivas R. Popuri[d], Mihai-Cosmin Pascariu[a,e], Mircea Niculescu[c], Radu Banica[a,c,*]

[a] *National Institute of Research & Development for Electrochemistry and Condensed Matter – INCEMC Timisoara, 144 Dr. Aurel Păunescu-Podeanu, RO-300569 Timisoara, Romania*

[b] *Institute of Applied Physics of the Academy of Sciences of Moldova, 5 Academiei, MD-2028 Chisinau, Moldova*

[c] *University Politehnica Timisoara, Faculty of Industrial Chemistry and Environmental Engineering, 6 Vasile Pârvan Blvd., RO-300223 Timisoara, Romania*

[d] *Institute of Chemical Sciences and Centre for Advanced Energy Storage and Recovery, School of Engineering and Physical Sciences, Heriot-Watt University, Edinburgh, EH14 4AS, UK*

[e] *"Vasile Goldis" Western University of Arad, Faculty of Pharmacy, 86 Liviu Rebreanu, RO-310414 Arad, Romania*

* Corresponding author. *E-mail address:* radu.banica@yahoo.com (R. Banica).

ACCEPTED MANUSCRIPT

Graphical Abstract

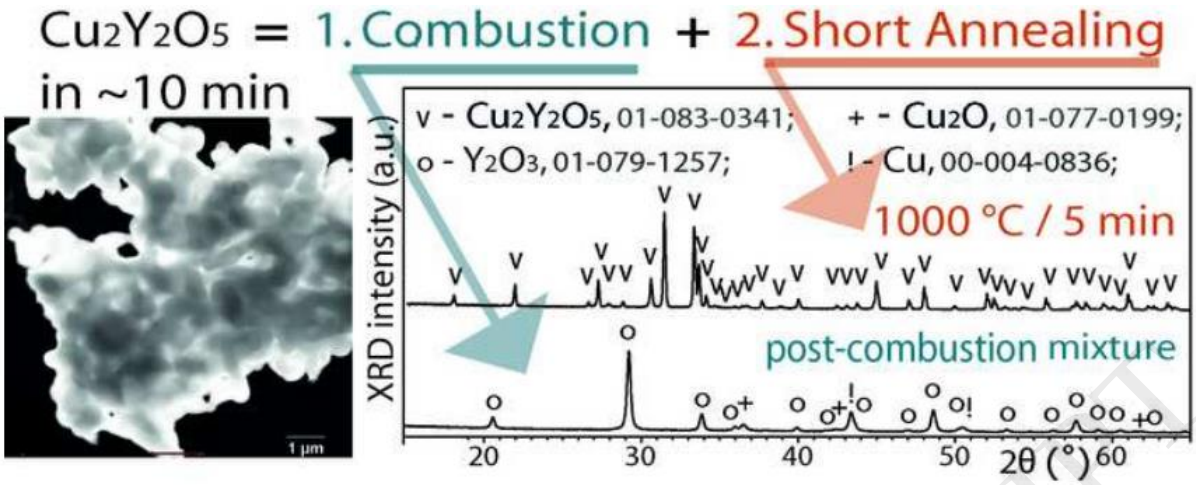

Highlights

- A simple, rapid and energy saving combustion synthesis of $Cu_2Y_2O_5$ microcrystals.
- Short combustion time < 1 s ensures the obtaining of a reactive precursor mixture.
- The liquid phase combustion ensures a good homogeneity of precursors.
- The optimal annealing time at 1000 °C for pure phase $Cu_2Y_2O_5$ is around 5 minutes.
- The vacuum HT-XRD study reveals the conversion of $Cu_2Y_2O_5$ into $CuYO_2$ delafossite.

ABSTRACT

A rapid synthesis method of $Cu_2Y_2O_5$ micropowders, which takes around 10 minutes, is reported for the first time. This fast procedure, achieved by combining a nitrate/glycerol auto-combustion and an annealing step, constitutes an important improvement over the conventional solid-state reaction methods, which usually require several hours. The analysis of products was performed using X-ray diffraction, scanning electron microscopy, high-resolution transmission electron microscopy, scanning transmission electron microscopy, Fourier transform Raman spectroscopy and diffuse reflectance spectroscopy. The optical band gap of $Cu_2Y_2O_5$, estimated using the Tauc plot, was found to be 2.58 eV. The high-

ACCEPTED MANUSCRIPT

temperature X-ray diffraction study, which was performed in a vacuum, confirmed the conversion of the $Cu_2Y_2O_5$ phase to a mixture of $CuYO_2$ delafossite and Y_2O_3. Thus, the overall time for obtaining $CuYO_2$, which is a well-known transparent conducting oxide (TCO), can be reduced to under 1 hour.

Keywords:

Auto-combustion reaction

Short annealing

Micropowder

Transparent conducting oxide

High-temperature XRD

1. Introduction

Copper-based ternary oxides, such as $Cu^{II}_2M^{III}_2O_5$ and $Cu^{I}M^{III}O_2$ delafossites, have gained tremendous interest due to their great potential in several important technologies, including superconducting compounds in the Cu-M-Ba-O system [1] and p-type transparent conducting oxides (TCO), like $CuYO_2$ [2-4]. K.T. Jacob *et al.* and G.M. Kale *et al.* have made significant contributions to the studies regarding the synthesis of compounds in the Cu-M-O system, establishing the phase relations, the decomposition temperatures and the correlation of thermodynamic properties with the ionic radius of the trivalent rare-earth cations for such compounds [1,5-9]. The Gibbs free energies of formation and the phase equilibria between $Cu_2Y_2O_5$ and $CuYO_2$ have also been investigated [10,11]. The crystalline structure of $Cu_2M_2O_5$ compounds was identified to belong to the orthorhombic system with the space group *P*21*nb*, consisting of an orthorhombic framework of MO_6 polyhedra, with the

ACCEPTED MANUSCRIPT

copper ions being surrounded by a highly deformed octahedron composed of oxygen ions [12,13].

$Cu_2Y_2O_5$ is a less studied compound, due to its modest direct applications. Some studies on its magnetic [13-16,17], thermal [18,19] and optical [20,21] properties have been performed, which may lead to photocatalytic [22,23] and antibacterial coatings [24,25] applications. However, its most noticeable use during the last decade was as a precursor for the synthesis of $CuYO_2$ delafossite [26-29], which was mentioned for the first time by M. Kato *et al.* in 1983 [30]. The established method for synthesizing $Cu_2Y_2O_5$ powders involves a solid state reaction, performed by heating copper and yttrium oxides at elevated temperatures, between 800 and 1200 °C [26,28,31]. The total synthesis time, required for the formation of the pure phase, is of the order of several hours, i.e. 3 h [28], 5 h [31], 6 h [25] or 24 h [26]. On the other hand, the wet-chemical synthesis methods, such as auto-combustion, co-precipitation, sol-gel, hydrothermal and solvothermal synthesis, have proven to be more effective for obtaining pure-phase materials, because they require a lower reaction temperature and duration.

In order to reduce the overall time and energy consumption for obtaining microcrystalline $Cu_2Y_2O_5$, we have developed a novel method which reduces the synthesis time from a few hours to 10 minutes. A subsequent annealing study, which confirmed the rapid conversion of $Cu_2Y_2O_5$ to a mixture of $CuYO_2$ delafossite and Y_2O_3, was performed and is also reported in this paper.

2. Experimental

2.1. Rapid synthesis of $Cu_2Y_2O_5$

ACCEPTED MANUSCRIPT

Analytical grade metal nitrates and methanol were purchased from Sigma-Aldrich, while glycerol was purchased from Chimreactiv (Romania). The synthesis started with the preparation of a 1.79 mol L^{-1} glycerol solution, using methanol as solvent. In the first step (Fig. 1), stoichiometric amounts of $Y(NO_3)_3 \cdot 6H_2O$ and $Cu(NO_3)_2 \cdot 3H_2O$ were dissolved in 5.0 mL of glycerol solution under continuous stirring, after which the obtained deep blue solution was heated to reach the ignition temperature (128 °C). In the second step, the powdery product, obtained after the liquid's combustion, was placed in alumina crucibles and heated in air at temperatures between 800 and 1000 °C for 5, 10 or 30 minutes. The crucibles were directly introduced into the furnace, which was preheated at the working temperature. Following the annealing, the crucibles were cooled to room temperature in 5-10 min. The thus-prepared powder samples were used for further characterization and for vacuum decomposition to $CuYO_2$ in a third step.

2.2. Analytical methods

The auto-ignition temperature was determined using a PC interfaced PCE-892 thermometer with a K-type thermocouple.

The phase purity of the as-synthesized powders was investigated with a X'Pert PRO X-ray powder diffractometer, by using Ni-filtered Cu Kα radiation (λ = 1.54 Å) and a 4 h/sample measurement time (0.013° 2θ step, time per step: 445.39 s). Profile matching to the XRD pattern was performed using the pseudo-Voigt Axial divergence asymmetry profile function in the FullProf Suite. The average crystallite sizes (L) of $Cu_2Y_2O_5$ powders were estimated using the Debye-Scherrer equation; the line broadening of the diffractometer was measured using a polycrystalline silicon standard. Also, the $CuYO_2$ phase formation from

ACCEPTED MANUSCRIPT

$Cu_2Y_2O_5$ was studied using the in-situ high-temperature XRD technique, in the 400-1000 °C domain, with a 100 °C step and a 10 min/acquisition measurement time.

The Fourier transform Raman data were collected with a SpectraPro–2500i spectrometer, using a 532 nm excitation wavelength.

The diffuse reflectance spectroscopy (DRS) data were acquired using a Lambda 950 UV/VIS/NIR spectrophotometer, with a 150 mm integrating sphere (Spectralon was used as the reflectance reference).

Scanning electron microscopy (SEM) images were acquired using a FEI Inspect S microscope while scanning transmission electron microscopy (STEM) and high-resolution transmission electron microscopy (HRTEM) micrographs were obtained using a Titan G2 80-200.

3. Results and discussion

3.1. $Cu_2Y_2O_5$ micropowder

3.1.1. Formation mechanism

The synthesis of $Cu_2Y_2O_5$ was achieved through the auto-combustion of a mixture consisting of yttrium and copper nitrates in a glycerol/methanol solution, followed by an additional thermal treatment (see section 2.1 and Fig. 1).

The XRD patterns of the as-obtained and annealed (at various temperatures) powders are shown in Fig. 2. The post-combustion reaction product consists of a mixture of Y_2O_3, Cu_2O, and traces of Cu.

ACCEPTED MANUSCRIPT

The combustion process for the metal nitrates/glycerol mixture is represented in Fig. 3. At first, the methanol vaporizes, after which a quantity of water from the hydrated metal salts is lost as well. During these processes, the solution viscosity increases and the color of the solution changes from deep blue to greenish-blue. Foaming is observed near the ignition point. The combustion reaction, which starts at 128 °C, is accompanied by a flame.

Assuming that enough dioxygen would be present in the system during the reaction, the glycerol combustion could be represented according to the following equations:

$$3CO_2 + 14e^- + 14H^+ \rightleftharpoons C_3H_8O_3 + 3H_2O \quad \text{(Equation 1)}$$

$$NO_3^- + 3e^- + 4H^+ \rightleftharpoons NO + 2H_2O \quad \text{(Equation 2)}$$

$$O_2 + 4e^- + 4H^+ \rightleftharpoons 2H_2O \quad \text{(Equation 3)}$$

$$C_3H_8O_3 + 2NO_3^- + 2O_2 + 2H^+ \rightarrow 3CO_2 + 2NO + 5H_2O \quad \text{(Equation 4)}$$

$$2NO + O_2 \rightarrow 2NO_2 \quad \text{(Equation 5)}$$

In our case, most of the oxygen required for combustion is released during the decomposition of yttrium and copper nitrates, so the overall reaction between the nitrates and glycerol can be written as:

$$14Y(NO_3)_3 \cdot 6H_2O + 14Cu(NO_3)_2 \cdot 3H_2O + 25C_3H_8O_3 + 70O_2 \rightarrow$$

$$7Cu_2Y_2O_5 + 70NO_2 + 75CO_2 + 226H_2O \quad \text{(Equation 6)}$$

A part of the hydration water from the metal nitrates vaporizes before reaching the ignition temperature. Afterwards, the decomposition of copper and yttrium nitrates occurs at different temperatures. As seen from literature, the Y_2O_3 formation by thermal decomposition

ACCEPTED MANUSCRIPT

of $Y(NO_3)_3 \cdot 6H_2O$ takes place in nine stages [32]. The most endothermic processes take place at temperatures between 300 and 500 ºC and are associated with the loss of hydration water. The Y_2O_3 compound is formed only at temperatures higher than 450 ºC, according to the chemical reaction's equation: $2Y_4O_5(NO_3)_2 \rightarrow 4Y_2O_3 + 4NO_2 + O_2$ [32].

If we use a stoichiometric mixture of nitrates and glycerol at temperatures lower than 450 ºC, the reducing conditions are present in the system. Due to this, the reduction of Cu^{II} to Cu^{I}, followed by Cu^0, occurs, as noticed from the XRD pattern of the post-combustion mixture (Fig. 2). This means that a part of the oxygen released during the nitrates' (i.e. $Y_4O_4(NO_3)_4$ and $Y_4O_5(NO_3)_2$) decomposition [32] does not react with the fuel. According to Equation 6, 53 moles of gases are released for each mole of $Cu_2Y_2O_5$. This high volume of gases hinders the access of oxygen from the ambient air. In this way, the reoxidation of metallic Cu and of Cu_2O to CuO is also hindered. As a result of the combustion reaction, the formation of $Cu_2Y_2O_5$ does not take place directly, due to the very short time (under one second) of precursors' exposure to elevated temperatures (Fig. 3). In order to compensate for this, we performed a subsequent thermal treatment on the obtained foam mixture.

At high temperatures, both Cu_2O and Cu oxidize to CuO, which further reacts with Y_2O_3 in an oxidizing atmosphere to form $Cu_2Y_2O_5$ [14]. From the change in the Gibbs free energy, corresponding to the reaction between Y_2O_3 and CuO, it is possible to conclude that a spontaneous reaction only occurs at temperatures higher than 673 °C [10]. It was also observed that orthorhombic $Cu_2Y_2O_5$ is present as a minority phase in the mixture with cubic Y_2O_3 and CuO at 700 °C [33].

Because of the low reaction rate at 700 °C, the annealing of the reaction mixture was performed at 800 ºC and 900 ºC for 30 minutes and, respectively, at 900 ºC and 1000 ºC for 5 and 10 minutes. After annealing the post-combustion mixture at 800 °C for 30 minutes, the XRD pattern shows the two phases corresponding to $Cu_2Y_2O_5$ and Y_2O_3, indicating an

ACCEPTED MANUSCRIPT

incomplete reaction (Fig. 2, marked with a black arrow). By increasing the annealing temperature to 900 °C, after 5 minutes, the Y_2O_3 concentration is reduced (Fig. 2, gray arrow). Traces of Y_2O_3 can be seen in the XRD pattern even after increasing the annealing time to 30 minutes at 900 °C (Fig. 2, light gray arrow). In order to obtain the pure phase material, the temperature was further increased to 1000 °C and the annealing time was reduced to 10 or 5 minutes. The latter annealing parameters were found to be the optimal conditions for obtaining $Cu_2Y_2O_5$ as a pure phase.

3.1.2 Structural studies

At room temperature, all XRD reflections of the synthesized $Cu_2Y_2O_5$ closely match with the ones from ICDD file 01-83-0341. No traces of other phases corresponding to any yttrium or copper oxides were detected. The crystal structure was refined in order to determine the lattice parameters, the XRD pattern of $Cu_2Y_2O_5$ prepared at 1000 °C for 5 minutes being analyzed with profile matching (Fig. 4). All diffraction reflections were indexed according to the orthorhombic phase of $Cu_2Y_2O_5$ with space group P*na*21 (33), with lattice parameters a = 10.8006(1) Å, b = 3.4962(1) Å, c = 12.4539(1) Å and V = 470.282(8) Å.

The average crystallite sizes (L) of $Cu_2Y_2O_5$ powders were estimated using the Debye-Scherrer equation,

$$L = \frac{K\lambda}{\beta \cos\theta} \qquad \text{(Equation 7)}$$

where K is a constant related to the crystallite shape and taken as 0.9 (assuming that the crystallites are spherical in shape), λ is the X-ray wavelength, β is the line broadening of the peak at half of the maximum intensity (FWHM) after subtracting the instrumental line broadening, and θ is the Bragg angle. For the average crystallite size estimation, the XRD

ACCEPTED MANUSCRIPT

peak at 2θ=31.287 degrees (the (211) Bragg reflection) was used. The calculated average crystallite size of $Cu_2Y_2O_5$ particles obtained at 800 °C/30 min, 900 °C/5 min, 900 °C/30 min and 1000 °C/5 min are 111, 109, 129 and 180 nm, respectively. This shows that an increase in the reaction temperature or duration leads to an enhancement in the crystallites' sizes.

3.1.3. Morphological studies

The morphology images of the $Cu_2Y_2O_5$ product, obtained at 1000 °C after 5 minutes of thermal treatment, shows microparticles having a foam aspect (Fig. 5a). Due to the high-temperature combustion reaction, individual microcrystals become attached to each other, forming aggregates. An interplanar distance of about 4.08 nm was measured using HRTEM for ten atomic layers, as shown in Fig. 5b. This corresponds to the (202) crystallographic plane of $Cu_2Y_2O_5$. STEM images, showing agglomerations of $Cu_2Y_2O_5$ particles, are presented at two magnification in Fig. 6. Some of these particles have sizes close to those estimated with the Scherrer equation for single crystallites of the same compound, around 180 nm, and are thus probably composed of a single crystallite.

3.1.4. Optical properties

The phase purity of $Cu_2Y_2O_5$ was also investigated using Fourier transform Raman spectroscopy. A typical ambient temperature Raman spectrum of a sample (1000 °C/5 min variant) is shown in Fig. 7. The Raman spectrum shows several sharp peaks corresponding to the lattice vibrations. The predominant Raman lines, located around 157, 173, 199, 210, 241, 264, 302, 328, 354, 393, 515, 562 and 586 cm^{-1}, are in agreement with the values reported in

ACCEPTED MANUSCRIPT

literature [31]. The Raman spectroscopy also confirms the phase purity of $Cu_2Y_2O_5$, as there is no trace of Y_2O_3 (band at 376 cm^{-1}), which is in agreement with the XRD data.

The optical properties of $Cu_2Y_2O_5$ were also investigated using DRS (Fig. 8). The bluish-green color of the samples, characteristic for compounds of this type, is due to the crystal field splitting of Cu^{2+} d-orbitals and the $^2T_{2g} \leftarrow {}^2E_g$ electronic transition [20]. The broad peak in the 350–600 nm spectral range, with the maximum at 498 nm, shows a spectral shape close to the one already reported [20,22]. In order to estimate the optical band gap, the Tauc plot, $(F(R)hv)^{2/n}$ vs hv, was used, in which $F(R)$ is the Kubelka-Munk absorbance, hv is the photon energy, and $n = 1$ for allowed direct optical transitions. The optical band gap (E_g) value was taken at the intersection point of the traced tangent and the horizontal hv axis. As shown in Fig. 8 (inset), in the case of $Cu_2Y_2O_5$ prepared at 1000 °C for 5 min, the direct band gap is estimated to be 2.58 eV. The 0.10 eV deviation from the already reported bandgap value of 2.48 eV for $Cu_2Y_2O_5$ powder material [22] can be attributed to the different method of estimation used; the well-established Tauc plot for band gap estimations, which we have used in this paper, is generally known to give more accurate results.

3.2. $CuYO_2$ phase formation

Obtaining $Cu_2Y_2O_5$ is an important intermediate step in the formation of $CuYO_2$ delafossite [26,30]. Therefore a high-temperature XRD study on the obtained $Cu_2Y_2O_5$ powders was performed in order to identify favorable synthesis conditions and time for preparation of $CuYO_2$.

In spite of an earlier study regarding the $CuYO_2$ formation by annealing of $Cu_2Y_2O_5$ at 1020°C in air [34], the recent studies reveal that $Cu_2Y_2O_5$ decomposes into Y_2O_3, Cu_2O and CuO at 1100 °C in air, without forming the $CuYO_2$ phase [28]. This is attributed to the low

ACCEPTED MANUSCRIPT

thermodynamic driving force involved in the formation of $CuYO_2$. As a consequence, an inert atmosphere would be a necessary condition for delafossite phase formation, in order to avoid its decomposition. The studied phase transformation conditions included a 10^{-2} mbar vacuum and a 10 min/scan exposure time at temperatures in the 400-1000 °C domain (Fig. 9). We have observed that $Cu_2Y_2O_5$ is stable up to 500 °C and that the phase conversion of $Cu_2Y_2O_5$ starts above this temperature. Up to 700 °C, a phase coexistence of $Cu_2Y_2O_5$, $CuYO_2$ and Y_2O_3 is noticed. Above 800 °C, only traces of $Cu_2Y_2O_5$ can be observed, which indicates the complete transformation of $Cu_2Y_2O_5$ into $CuYO_2$ and Y_2O_3 phases. These results suggest that it is possible to obtain $CuYO_2$ delafossite in vacuum above 700 °C under 50 min. However, further investigations to obtain a pure $CuYO_2$ phase are necessary. Also some literature data confirms that the decomposition of $Cu_2Y_2O_5$ to $CuYO_2$ in argon atmosphere at 900 °C can be achieved in around 10 min [21].

4. Conclusions

The efficiency of our rapid two-step technique for the production of $Cu_2Y_2O_5$ microcrystals in 10 minutes was demonstrated. The first step of this technique, namely the auto-combustion synthesis, leads to the formation of a mixture of Y_2O_3, Cu_2O, and Cu. The second step consists in the annealing of the post-combustion product at 1000 °C for 5 minutes. In this way, the oxidation of Cu_2O and Cu leads to the formation of CuO, which reacts with Y_2O_3, allowing for the formation of pure phase $Cu_2Y_2O_5$. The crystallites' dimensions estimated using the Scherrer equation were around 180 nm for the $Cu_2Y_2O_5$ microparticles, which were confirmed by STEM. XRD data, Fourier transform Raman spectroscopy and HRTEM confirmed the purity of the synthesized materials. Using the Tauc plot, the value of the band gap for $Cu_2Y_2O_5$ was estimated to be 2.58 eV. The high-

ACCEPTED MANUSCRIPT

temperature X-ray diffraction study, performed in a vacuum in the third step, confirmed the $Cu_2Y_2O_5$ phase conversion to a mixture of $CuYO_2$ delafossite and Y_2O_3. This result allows the overall time required for synthesis of delafossite to be reduced to under 1 hour.

Acknowledgements

This work was partially supported by the grant POSDRU/159/1.5/S/137070 (2014) of the Ministry of National Education, Romania, co-financed by the European Social Fund – Investing in People, within the Sectoral Operational Programme Human Resources Development 2007-2013. We thank Dr. Olga Iliasenco and Daniela Drasovean for their help in drafting the paper.

ACCEPTED MANUSCRIPT

References

[1] K.T. Jacob, T. Mathews, J.P. Hajra, Gibbs' Free Energies of Formation of $Cu_2Ln_2O_5$ (Ln = Tb, Dy, Er, Yb) Compounds, High Temp. Mater. Processes (Berlin, Ger.) 12 (1993) 251-258, https://doi.org/10.1515/HTMP.1993.12.4.251.

[2] T. Ehara, Preparation of $CuYO_2$ Thin Films by Sol-Gel Method Using Copper Acetate and Yttrium Acetate as Metal Sources, J. Mater. Sci. Chem. Eng. 4 (2016) 24-28, http://dx.doi.org/10.4236/msce.2016.41005.

[3] A.N. Banerjee, K.K. Chattopadhyay, Recent developments in the emerging field of crystalline p-type transparent conducting oxide thin films, Prog. Cryst. Growth Charact. Mater. 50 (2005) 52-105, http://dx.doi.org/10.1016/j.pcrysgrow.2005.10.001.

[4] M.A. Marquardt, N.A. Ashmore, D.P. Cann, Crystal chemistry and electrical properties of the delafossite structure, Thin Solid Films 496 (2006) 146-156, https://doi.org/10.1016/j.tsf.2005.08.316.

[5] K.P. Jayadevan, K.T. Jacob, Stability of $Cu_2Ln_2O_5$ Compounds - Comparison, Assessment and Systematics, High Temp. Mater. Processes (Berlin, Ger.) 19 (2000) 389-397, https://doi.org/10.1515/HTMP.2000.19.6.389.

[6] T. Mathews, K.T. Jacob, Phase relations in the systems Cu–O–R_2O_3 (R = Tm, Lu) and Gibbs energies of formation of $Cu_2R_2O_5$ compounds, J. Mater. Chem. 3 (1993) 1025-1029, https://doi.org/10.1039/JM9930301025.

[7] G.M. Kale, Gibbs Energy of Formation of $Cu_2Yb_2O_5$ and Thermodynamic Stability of $Cu_2R_2O_5$ (R = Tb-Lu), J. Solid State Chem. 125 (1996) 13-18, https://doi.org/10.1006/jssc.1996.0258.

ACCEPTED MANUSCRIPT

[8] G.M. Kale, R.V. Kumar, D.J. Fray, Gibbs energy of formation of $Cu_2R_2O_5$ (R = Dy, Ho, Er, Yb) from component oxides employing solid oxide electrochemical cells, Solid State Ionics 86-88 (1996) 1421-1425, https://doi.org/10.1016/0167-2738(96)00324-4.

[9] G.M. Kale, K.T. Jacob, Gibbs energies of formation of $CuYO_2$ and $Cu_2Y_2O_5$ and phase relations in the system Cu-Y-O, Chem. Mater. 1 (1989) 515-519, https://doi.org/10.1021/cm00005a010.

[10] W. Przybyło, K. Fitzner, Gibbs free energy of formation of the solid phases $Cu_2Y_2O_5$ and $CuYO_2$ determined by the E.M.F. method, Thermochim. Acta 264 (1995) 113-123, http://dx.doi.org/10.1016/0040-6031(95)02412-U.

[11] R.A. Konetzki, R. Schmid-Fetzer, Oxygen Coulometric Investigation of the Y-Cu-O System, J. Solid State Chem. 114 (1995) 420-427, https://doi.org/10.1006/jssc.1995.1064.

[12] J.L. García-Muñoz, J. Rodríguez-Carvajal, Structural Characterization of $R_2Cu_2O_5$ (R = Yb, Tm, Er, Y, and Ho) Oxides by Neutron Diffraction, J. Solid State Chem. 115 (1995) 324-331, https://doi.org/10.1006/jssc.1995.1141.

[13] M. Baran, R. Szymczak, R.Z. Levitin, B.V. Mill, Anisotropy of magnetic properties of $R_2Cu_2O_5$ cuprates (R=Y, Lu, Tm, Yb, Tb), J. Exp. Theor. Phys. 82 (1996) 518-523.

[14] J. Typek, N. Guskos, Magnetic low dimensional effects in $(Dy_{0.375}Y_{0.625})_2Cu_2O_5$ studied by ESR spectroscopy, Rev. Adv. Mater. Sci. 12 (2006) 106-111.

[15] J. Typek, Competing interactions and dimensional crossover in $(Er_{0.5}Y_{0.5})_2Cu_2O_5$ studied by EPR, J. Alloys Compd. 440 (2007) 26-29, https://doi.org/10.1016/j.jallcom.2006.09.076.

[16] B.L. Ramakrishna, E.W. Ong, Z. Iqbal, Magnetic properties of $Y_2Cu_2O_5$, Solid State Commun. 68 (1988) 775-779, https://doi.org/10.1016/0038-1098(88)90062-2.

ACCEPTED MANUSCRIPT

[17] U. Adem, G. Nénert, Arramel, N. Mufti, G.R. Blake, T.T.M. Palstra, Magnetodielectric coupling by exchange striction in $Y_2Cu_2O_5$, Eur. Phys. J. B (2009) 71: 393-399, https://doi.org/10.1140/epjb/e2009-00209-1.

[18] L.T. Denisova, L.G. Chumilina, V.M. Denisov, S.D. Kirik, S.A. Istomin, High-temperature heat capacity of $Y_2Cu_2O_5$, Phys. Solid State 56 (2014) 922-925, http://dx.doi.org/10.1134/S1063783414050072.

[19] V.V. Moshchalkov, N.A. Samarin, I.O. Grishchenko, B.V. Mill, Y. Zoubkova, Low temperature specific heat of $R_2Cu_2O_5$ (R = Y, Tb, Dy, Ho, Er, Tm, Yb, Lu) compounds, J. Magn. Magn. Mater. 90-91 (1990) 533-535, https://doi.org/10.1016/S0304-8853(10)80195-7.

[20] J.K. Kar, R. Stevens, C.R. Bowen, Rare-earth cuprates for ceramic colouring application – An investigation, J. Alloys Compd. 455 (2008) 121-129, https://doi.org/10.1016/j.jallcom.2007.01.124.

[21] K.A. Vanaja, Growth and characterisation of p-type delafossite transparent conducting thin films for heterojunction applications (PhD thesis), Cochin University of Science and Technology, Kerala, India, 2011, pp. 94-101, https://dyuthi.cusat.ac.in/xmlui/handle/purl/2773.

[22] L. Zhang, J. Yan, M. Zhou, Y. Liu, Preparation, Characterization, and Enhanced Photocatalytic Hydrogen Evolution Activity of $Y_2Cu_2O_5$-Based Compounds under Simulated Sunlight Irradiation, J. Nanomater. 2013 (2013) Article ID 852139, http://dx.doi.org/10.1155/2013/852139.

[23] L. Zhang, K.L. Huang, H. Chen, J.H. Yan, Preparation and Modification of $Y_2Cu_2O_5/Y_2O_3$ Photocatalysts for H_2 Evolution under Simulated Sunlight Irradiation, Adv. Mater. Res. (Durnten-Zurich, Switz.) 239-242 (2011) 3001-3004, https://doi.org/10.4028/www.scientific.net/AMR.239-242.3001.

ACCEPTED MANUSCRIPT

[24] Y.P. Wang, T.W. Chiu, C.H. Chang, C. Xuan, G.J. Cheng, Transparent and antibacterial $Cu_2Y_2O_5$ thin films by chemical solution deposition, Thin Solid Films 570B (2014) 547-551, https://doi.org/10.1016/j.tsf.2014.02.033.

[25] T.W. Chiu, C.H. Chang, L.W. Yang, Y.P. Wang, Preparation of transparent $Cu_2Y_2O_5$ thin films by RF magnetron sputtering, Appl. Surf. Sci. 354A (2015) 110-114, https://doi.org/10.1016/j.apsusc.2015.02.129.

[26] B.J. Ingram, B.J. Harder, N.W. Hrabe, T.O. Mason, K.R. Poeppelmeier, Transport and Defect Mechanisms in Cuprous Delafossites. 2. $CuScO_2$ and $CuYO_2$, Chem. Mater., 16 (2004) 5623-5629, http://dx.doi.org/10.1021/cm048982k.

[27] G. Van Tendeloo, O. Garlea, C. Darie, C. Bougerol-Chaillout, P. Bordet, The Fine Structure of $YCuO_{2+x}$ Delafossite Determined by Synchrotron Powder Diffraction and Electron Microscopy, J. Solid State Chem. 156 (2001) 428-436, https://doi.org/10.1006/jssc.2000.9018.

[28] K. Nishio, T. Okada, N. Kikuchi, S. Mikusu, T. Iida, K. Tokiwa, T. Watanabe, T. Kineri, Preparation of delafossite $CuYO_2$ by metal-citric acid complex decomposition method, Mater. Res. Soc. Symp. Proc. 1166 (2009) 1166-N03-13, https://doi.org/10.1557/PROC-1166-N03-13.

[29] N. Tsuboi, K. Tosaka, S. Kobayashi, K. Kato, F. Kaneko, Preparation of Delafossite-Type $CuYO_2$ Films by Solution Method, Jpn. J. Appl. Phys. 47 (2008) 588-591, https://doi.org/10.1143/JJAP.47.588.

[30] T. Ishiguro, N. Ishizawa, N. Mizutani, M. Kato, A new delafossite-type compound $CuYO_2$: I. Synthesis and characterization, J. Solid State Chem. 49 (1983) 232-236, https://doi.org/10.1016/0022-4596(83)90117-2.

ACCEPTED MANUSCRIPT

[31] A. Bhargava, J.A. Alarco, G.J. Millar, R. Bell, T. Yamashita, I.D.R. Mackinnon, Fine-grained $Y_2Cu_2O_5$ powder from a co-precipitated precursor, Mater. Lett. 26 (1996) 89-96, https://doi.org/10.1016/0167-577X(95)00195-6.

[32] P. Melnikov, V.A. Nascimento, L.Z.Z. Consolo, A.F. Silva, Mechanism of thermal decomposition of yttrium nitrate hexahydrate, $Y(NO_3)_3 \cdot 6H_2O$ and modeling of intermediate oxynitrates, J. Therm. Anal. Calorim. 111 (2013) 115-119, https://doi.org/10.1007/s10973-012-2236-3.

[33] S. Götzendörfer, Synthesis of Copper-Based Transparent Conductive Oxides with Delafossite Structure via Sol-Gel Processing (PhD thesis), Universität Würzburg, Fakultät für Chemie und Pharmazie, 2010, pp. 82-87, https://opus.bibliothek.uni-wuerzburg.de/frontdoor/index/index/year/2011/docId/5134 (accessed 15.03.2017).

[34] A.J.S. Machado, R.F. Jardim, On the transformation of $Y_2Cu_2O_5$ into $YCuO_2$, Mater. Lett. 19 (1994) 177-183, https://doi.org/10.1016/0167-577X(94)90065-5.

ACCEPTED MANUSCRIPT

Figure captions

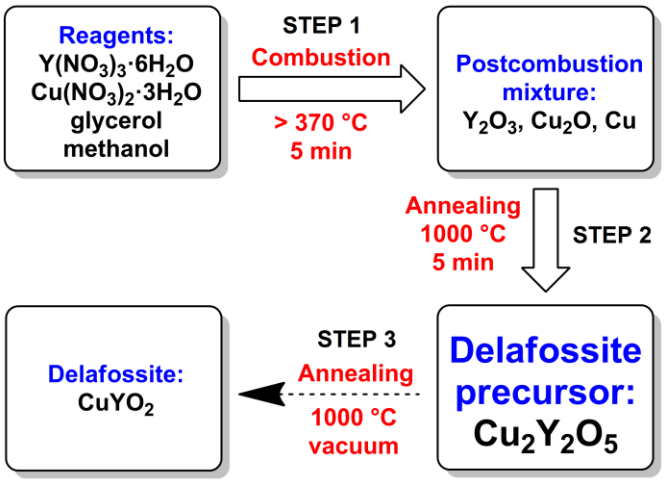

Fig. 1. General synthetic procedure for obtaining $Cu_2Y_2O_5$.

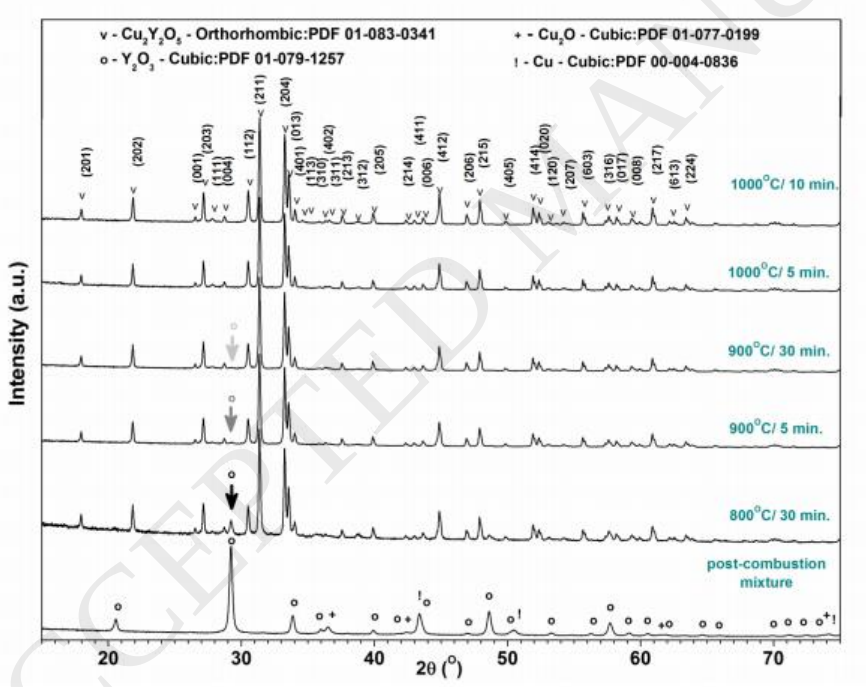

Fig. 2. XRD patterns of the post-combustion mixture and of the samples obtained at various annealing temperatures and durations.

ACCEPTED MANUSCRIPT

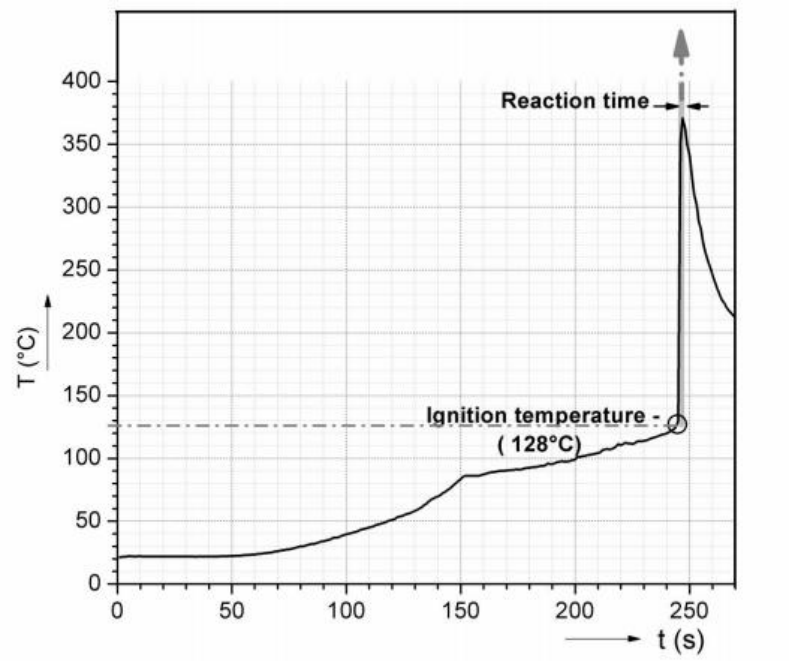

Fig. 3. Variation of the reacting system's temperature during the combustion of copper and yttrium nitrates dissolved in glycerol/methanol.

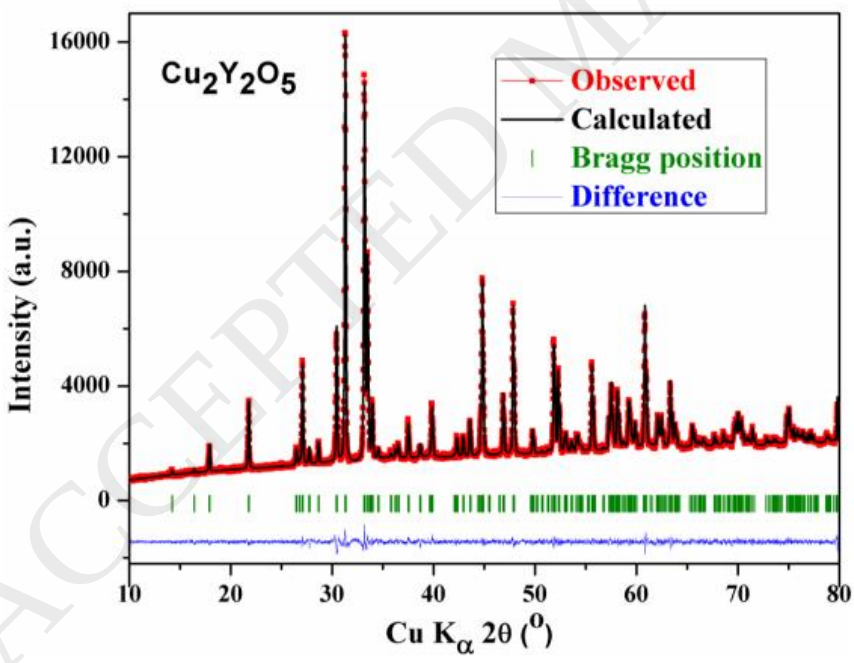

Fig. 4. Profile matching to the XRD pattern of $Cu_2Y_2O_5$ synthesized at 1000 °C/5 min; the observed (red points), calculated (black solid line), Bragg positions (green bars) and

ACCEPTED MANUSCRIPT

difference curve (bottom blue line) are shown; the conventional reliability factors for profile matching are R_p = 12.1 %, R_{wp} = 9.50 % and χ^2 = 1.787.

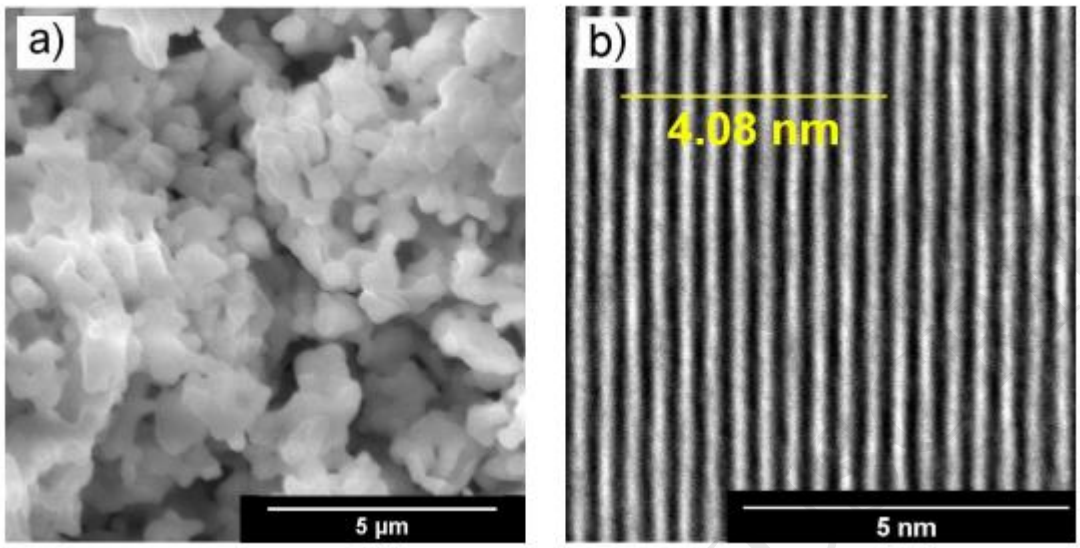

Fig. 5. SEM (a) and HRTEM (b) images of $Cu_2Y_2O_5$ annealed at 1000 °C for 5 min.

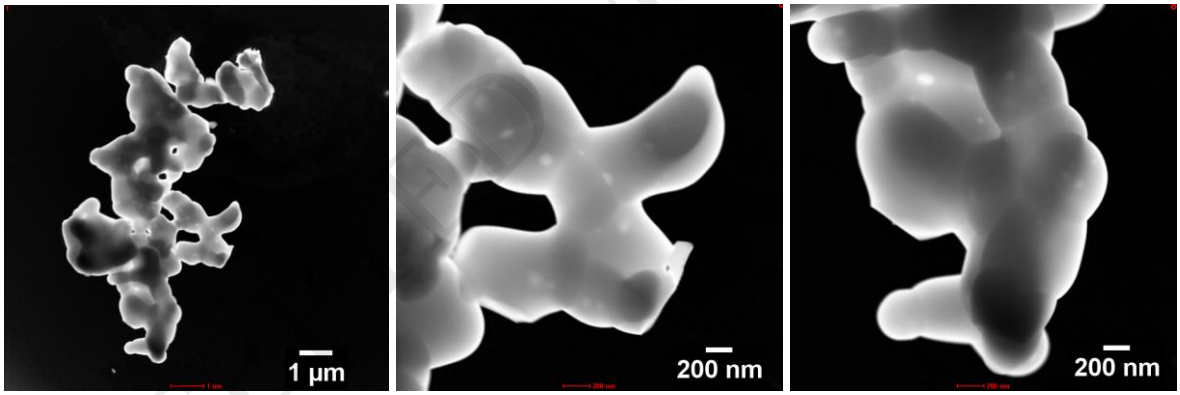

Fig. 6. STEM images of $Cu_2Y_2O_5$ annealed at 1000 °C for 5 min.

ACCEPTED MANUSCRIPT

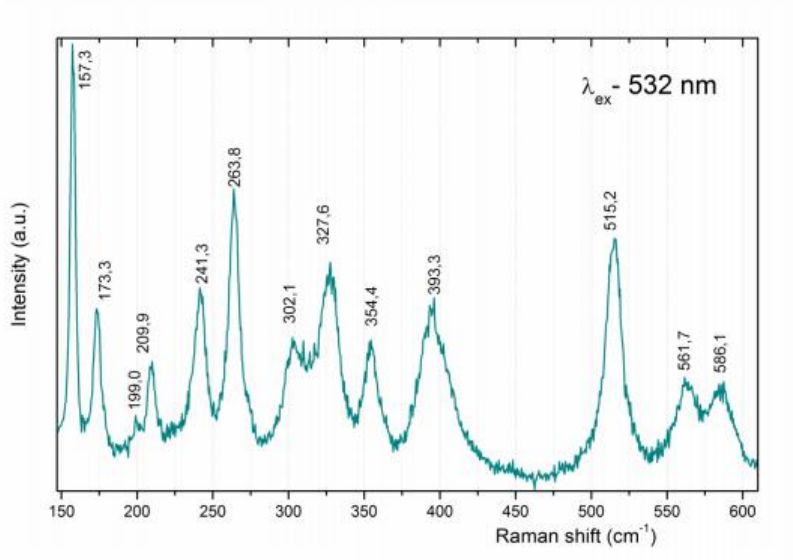

Fig. 7. Fourier transform Raman spectrum of $Cu_2Y_2O_5$ obtained at 1000 °C/5 min.

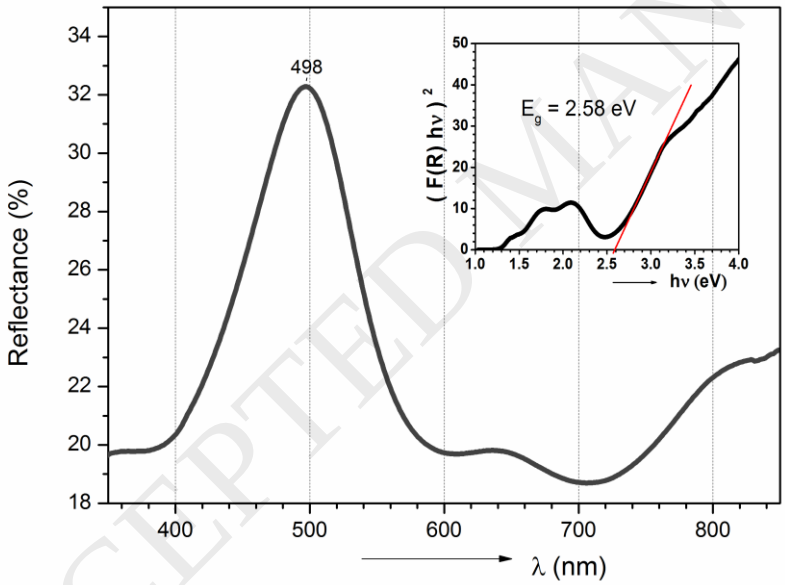

Fig. 8. DRS curve for $Cu_2Y_2O_5$ (inset: determination of the optical band gap of $Cu_2Y_2O_5$).

ACCEPTED MANUSCRIPT

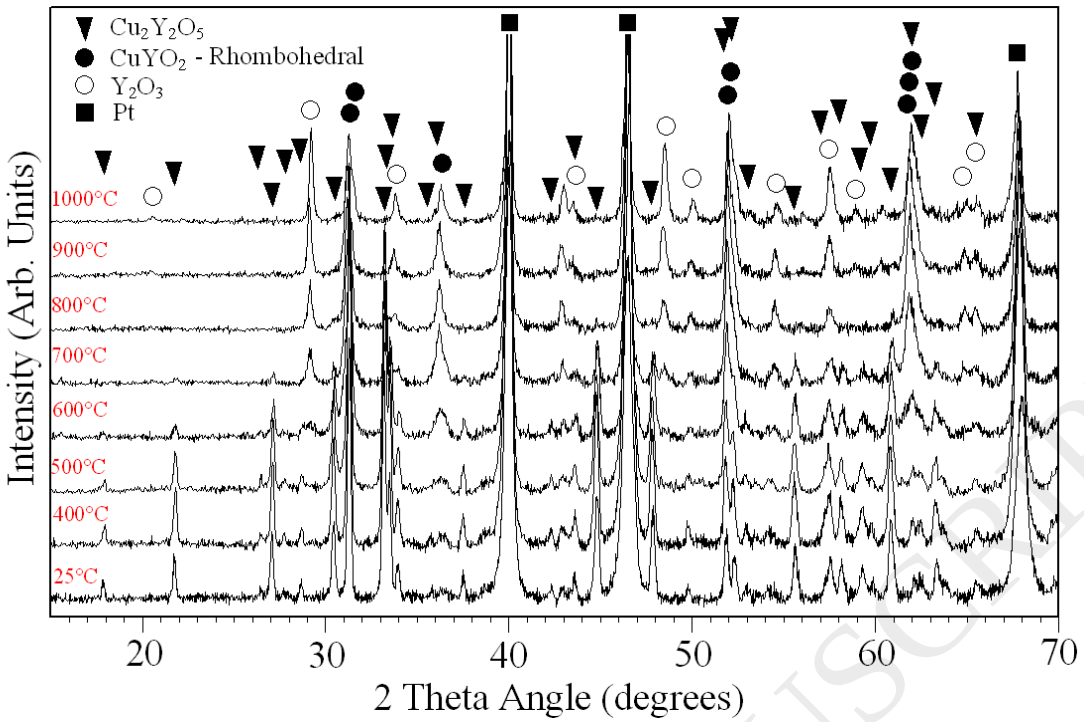

Fig. 9. High-temperature XRD patterns for decomposition of $Cu_2Y_2O_5$ in a vacuum (10^{-2} mbar).

ACCEPTED MANUSCRIPT